Towards Nanotube Linear Servomotors

doi: 10.1109/TASE.2006.875551

Towards Nanotube Linear Servomotors

Lixin Dong, *Member, IEEE*, Bradley J. Nelson, *Member, IEEE*, Toshio Fukuda, *Fellow, IEEE*, and Fumihito Arai, *Member, IEEE*

***Abstract*—Nanoscale linear servomotors with integrated position sensing are investigated from experimental, theoretical, and design perspectives. Prismatic motion is realized using the interlayer motion of telescoping multiwalled carbon nanotubes (MWNTs). Position sensing can be achieved by monitoring field emission or by measuring resistance change between an MWNT and a gold substrate during sliding movement. Experimental results demonstrate resolution in the nanometer range. Actuation experiments demonstrate the feasibility of a linear nanoservomotor with integrated position sensing based on field emission. A local "kink"-like fluctuation of emission current is observed, which is caused by the change of the protruding length of the nanotube core, thus demonstrating the potential of using emission as a "linear encoder." The complete extension of the inner core is observed and the electrostatic force is calibrated to be tens of nano-Newtons for individual nanotubes—16.5 nN under a 30-V bias. These results demonstrate the possibility of fabricating linear servomotors at the nanometer scale with integrated position sensing.**

***Note to Practitioners*—Nanometer scale actuators and sensors that can provide motion and measurement with nanometer-order resolution will enable new industrial applications in which only a few atoms or molecules are measured, transported, or processed. Linear servomotors will play a significant role in such applications because they provide precision prismatic motion directly without requiring a conversion from rotary to linear motion. Nano linear servomotors are experimentally and theoretically investigated in this paper. The devices take advantage of the ultra-low interlayer friction of a multiwalled carbon nanotube (MWNT). Position sensing feedback is achieved by monitoring field emission, which depends on interelectrode distance, or by measuring resistance change between an MWNT and a gold substrate during sliding movement. Whereas this paper targets long-term nanotechnology contributions, some intermediate results are ready for applications in the near future. The interlayer sliding motion demonstrated would enable the building of devices, such as Gigahertz oscillators and attolitter nanosyringes, and the sensors used for position feedback could find applications independently in a macro or microscale machine for detecting proximity, touch, displacement, or orientation.**

***Index Terms*—Carbon nanotube, field emission, linear servomotor, position sensing, telescoping nanotube.**

Manuscript received November 1, 2004; revised July 2, 2005. This paper was recommended for publication by Associate Editor W. Li and Editor M. Wang upon evaluation of the reviewers' comments.

L. Dong and B. J. Nelson are with the Institute of Robotics and Intelligent Systems, ETH Zürich, Zürich 8092, Switzerland (e-mail: ldong@ethz.ch; bnelson@ethz.ch).

T. Fukuda and F. Arai are with the Department of Micro-Nano Systems Engineering, Nagoya University, Nagoya 464-8603, Japan (e-mail: fukuda@mein.nagoya-u.ac.jp; arai@mein.nagoya-u.ac.jp).

Digital Object Identifier 10.1109/TASE.2006.875551

I. Introduction

THE generation of linear motion is important in both the technological world and in nature. Most machines are powered by internal combustion engines operating on the principle of linear alternating motion of a piston in a cylinder, or by motors actuated by transforming electric energy into mechanical motion. Among electric motors, linear servomotors play a significant role because they provide precision prismatic motion directly without requiring a conversion from rotary to linear motion which generally decreases efficiency and results in a larger and more complex mechanism.

In nature, prismatic motion related to intercellular exchanges, cell division, and muscle contraction is produced by protein linear motors [1]. Enzymes such as myosin, kinsin, and dynein are linear motors that move along polymer substrates and convert the energy liberated from adenosine triphosphate (ATP) hydrolysis into mechanical work; myosin moves along actin filaments in muscle and other cells, and kinesin and dynein along microtubules. Despite its ubiquity and versatility, protein has shortcomings as an engineering material. Protein machines are structurally flexible; they quit when dried, freeze when chilled, and cook when heated [2].

In 1992, Drexler discussed the possibility of constructing artificial nanomechanical rotary or linear motors with diamondoid covalent solids [3]. In the last decade, progress has been made in artificial nanoscale actuators due to the discovery of carbon nanotubes (CNTs) [4], nanowires [5], nanobelts [6], and other nanomaterials. Nanotubes produced in bulk have been used to fabricate actuators based on bond-length changes induced by charge injection [7]. Single wall carbon nanotube (SWNT)-Nafion composite actuators have been demonstrated for 0.1–18(%wt CNTs) doping of purified SWNTs within the polymer matrix. A 25 mm $\times$ 4 mm $\times$ 25 μm bimorph actuator was reported to deflect 4 mm [8]. Electrostatic deflection has also been shown for carbon nanotubes [9], [10]. Piezoelectric and ferroelectric zinc–oxide nanobelt-based structures have been synthesized and have potential as nanoscale actuator components [11]. While solid actuators can output relatively large forces, their stroke is generally proportional to their volume, which does not scale favorably for these dimensions. Another family of nano actuators resembling macroscale motors can be constructed by taking advantage of the ultra-low interlayer friction of a multiwalled nanotube (MWNT). Recently, a micro rotary actuator with a nanotube as a rotation bearing has been demonstrated [12].

Compared to protein linear motors, nanotube linear servomotors have potentially better controllability and can work in solid state, in a broader environment, such as in air or vacuum rather

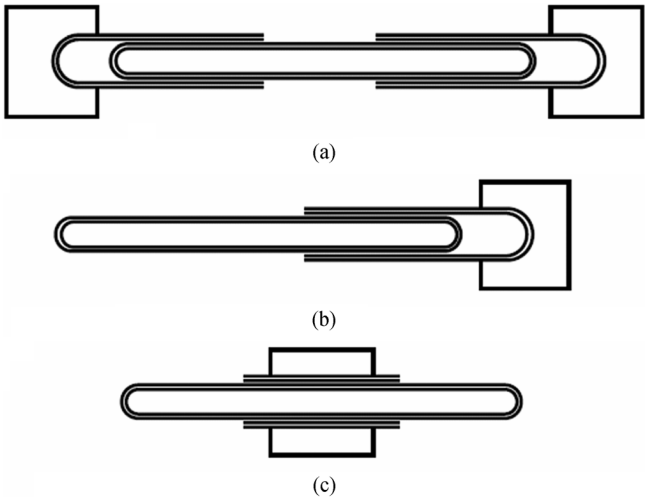

Fig. 1. Telescoping MWNTs. (a) Bridged telescoping MWNT (none opened end). (b) Cantilevered telescoping MWNT (one opened end). (c) Middle-supported telescoping MWNT (two opened ends).

than only in liquid, with changeable step sizes, and with potentially higher resolution. Protein linear motors may find applications in biotechnology and nanomedicines for molecule handling, drug delivery, and so on, whereas nanotube linear motors are designed for solid-state nanomachine actuation for such applications as atom/molecule manipulation and assembly.

To improve the precision of nanomotors, position sensing feedback is necessary. Although tunneling current and laser-deflection techniques can provide extremely high resolution feedback [13], [14], the effective distance of the former is less than 1 nm and the latter generally involves a complex laser apparatus. The dependence of field emission currents on interelectrode distance is another technique that may be used for position sensing. Recent results with nanotube emitters and telescoping nanotubes have shown the feasibility of this method [15], [16]. Another possible feedback mechanism is to use the interlayer resistance of a telescoping nanotube for position sensing [17]. The potential for quantized interlayer conductance can result in resolutions at atomic lattice-levels [18].

In the following, telescoping nanotubes are introduced in Section II. Actuation and position sensing are then presented in Sections III and IV, respectively. In Section V, an experiment with a linear nanomotor with integrated field emission current-based position sensing is described.

II. Telescoping Carbon Nanotubes

A. Overview

Telescoping structures obtained from MWNTs (Fig. 1) have evoked interest because of the possibility of their application in nanomechanical systems, such as ultra-low friction bearings [19]; gigahertz nanooscillators [20], [21]; and nanometer scale actuators. Based on their geometries, telescoping nanotubes can have zero, one, or two open ends as shown in Fig. 1. *In-situ* manipulation of the nanotube core allows controlled reversible telescoping and, furthermore, allows the associated forces to be quantified [22]. The steady-state resistance to interlayer sliding motion has been measured to be 0.08–0.3 MPa [23]. Robust ultralow-friction linear nanobearings and rotary microactuators

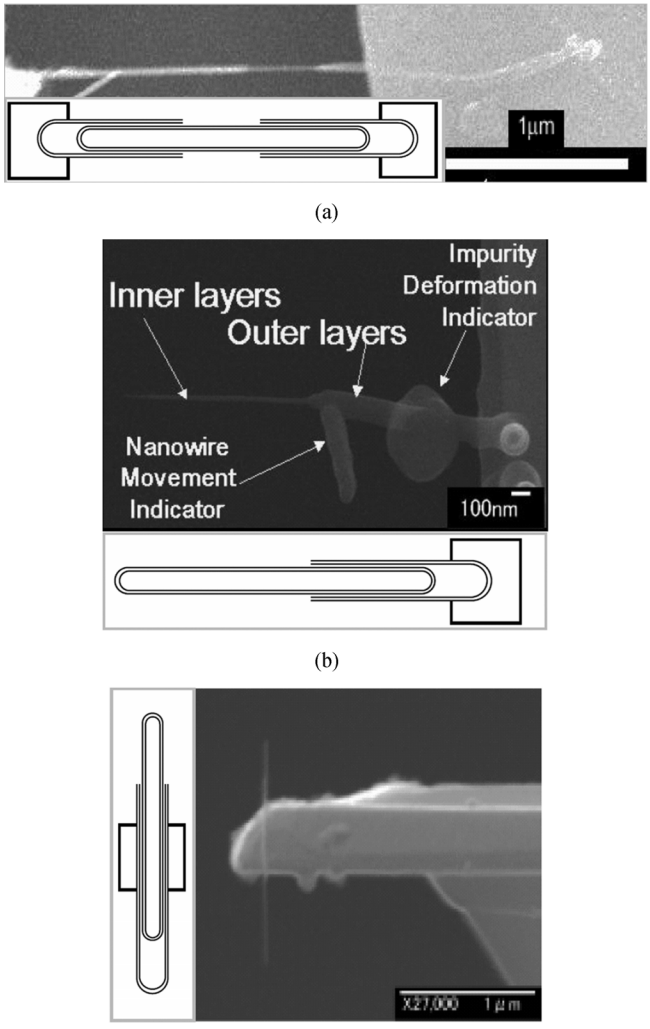

Fig. 2. Fabricated telescoping MWNTs. (a) Bridged telescoping MWNT. (b) Cantilevered telescoping MWNT. (c) Middle-supported telescoping MWNT.

have been demonstrated on the basis of an interlayer rotation of an MWNT [12].

B. Fabrication

Open-ended CNTs have been created by removing the commonly capped ends of MWNTs with acid etching [24], saturated current [25], electronic pulse [26], or mechanical strain [22], [27], thus providing access to inner-core nanotube cylinders. Acid etching is effective for opening nanotube caps but does not expose inner layers in a controlled way. Controlled fabrication with saturated current is potentially a large-scale manufacturing method, whereas electric pulse and mechanical strain are convenient *in-situ* processes.

C. Experimental Results

Here, we use mechanical pulling [27] to fabricate telescoping CNTs using nanorobotic manipulation techniques [28]. Typical examples are shown in Fig. 2 as bridged, cantilevered, and middle supported (with one open end) telescoping MWNTs. Fig. 2(a) shows a bridged telescoping MWNT with two ends fixed on a substrate (left end) and an atomic force microscope

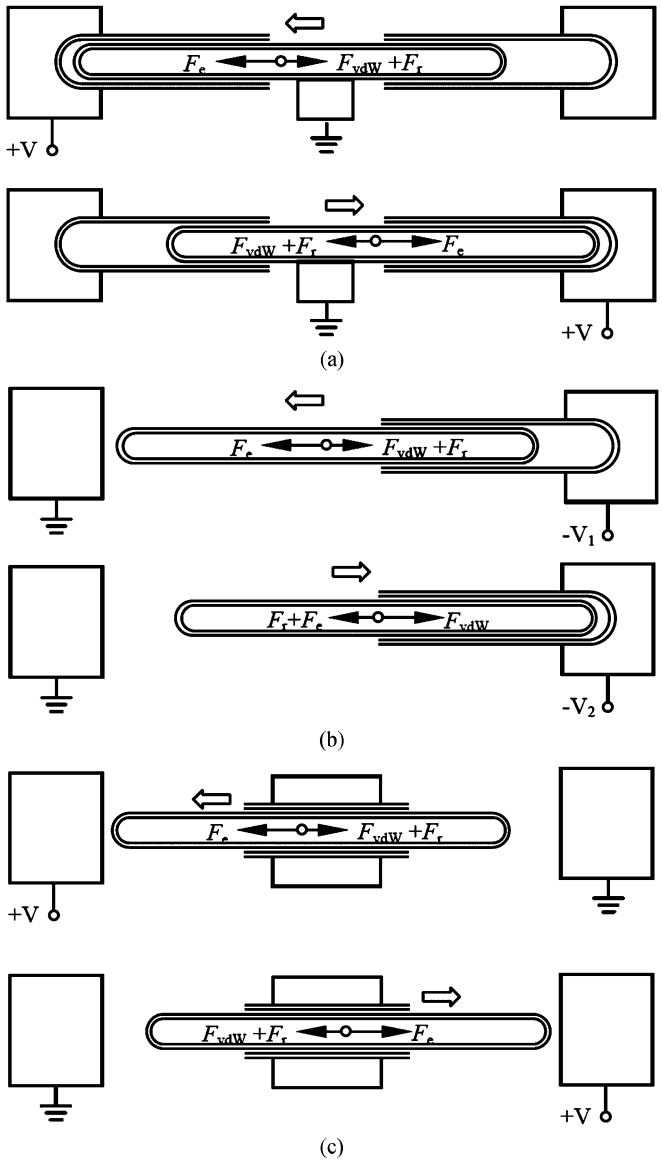

Fig. 3. Telescoping MWNT linear nanomotors. (a) Bridged telescoping MWNT prismatic nanomotor. (b) Cantilevered telescoping MWNT prismatic nanomotor. (c) Middle-supported telescoping MWNT linear nanomotor.

(AFM) cantilever (right end). The thinner neck of the bridged MWNT is formed by mechanical pulling (i.e., by moving the cantilever to the right so as to break the outer layer(s) and expose the inner ones as schematically shown in the inset). Fig. 2(b) shows a bridged telescoping MWNT formed with a similar process but moving the cantilever until the core is completely exposed. Similarly, if the nanotube is not fixed at the end but at the middle part on the cantilever, stress will occur only on a partial section. Fig. 2(c) shows a middle-supported telescoping MWNT being formed in this way. One end is kept capped, but can be opened if the process is repeated as shown in Fig. 2(b).

III. Actuation Using MWNTs

The configuration and mechanical models of linear nanomotors are shown in Fig. 3 based on (a) bridged, (b) cantilevered, and (c) middle-supported telescoping MWNTs. $F_{\rm e}$, $F_{\rm vdW}$, and

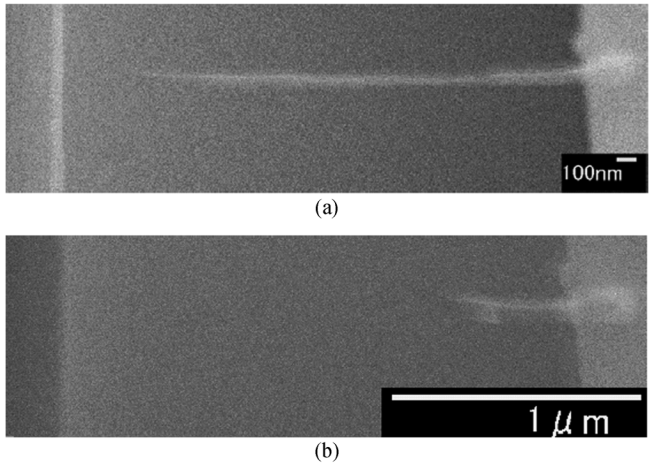

Fig. 4. Actuation experiments. Total protruding length of tube before actuation is 2126.3 nm and 467.5 nm after actuation. (a) Before actuation. (b) After actuation.

$F_{\rm r}$ denote electrostatic force, van der Waals interaction, and the total intershell sliding resistance force, respectively. The motion of the core section can be controlled by controlling the electrostatic force. Atomic scale mechanisms, such as interatomic locking, provide resistance to sliding the core in the outer tube, but experiments indicate that the intershell sliding resistance force between two neighboring shells of perfect or nearly perfect molecular structure is substantially smaller than the van der Waals restoring force. An experimental observation has shown an extruded core of a multiwalled carbon nanotube retract into the outer shells [19]. It has also been realized that the restoring force resulting from excess van der Waals interaction energies due to the core extrusion drives the core to oscillate with respect to its fully retracted position because of the small intershell sliding resistance force. The oscillation frequency can be in the gigahertz range [20], [29].

Actuation experiments also show that under lower bias voltages, it is possible to generate electrostatic forces that surpass the sum of the van der Waals interaction and atomic scale sliding resistance. Experimental results on a cantilevered telescoping nanotube (Fig. 4) verify this. As the core section is pulled out, the voltage increases from 20 to 30 V. This suggests that a relative low bias can generate an actuation force larger than the sum of the interlayer friction and van der Waals forces on the core of the telescoping MWNT. The electrostatic force can be estimated by monitoring the deflection of an AFM cantilever in an electron microscope. By resembling the system shown in Fig. 4, a nontelescoping MWNT is placed against an AFM cantilever by a manipulator installed in a transmission electron microscope (TEM) as shown in Fig. 5. The electrostatic force on the AFM cantilever has been detected to be 16.5 nN under a 30-V bias according to the deflection of the cantilever (550.4 nm), suggesting the upper limit of the interlayer friction and van der Waals forces of the telescoping nanotube shown in Fig. 4 to be smaller than this value.

IV. Position Sensing Using MWNTs

To realize controlled motion and to achieve high precision sliding of the core section, the position must be determined in

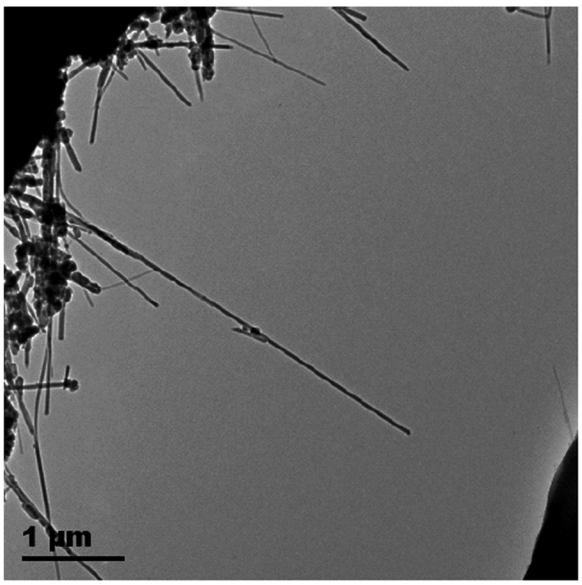

(a)

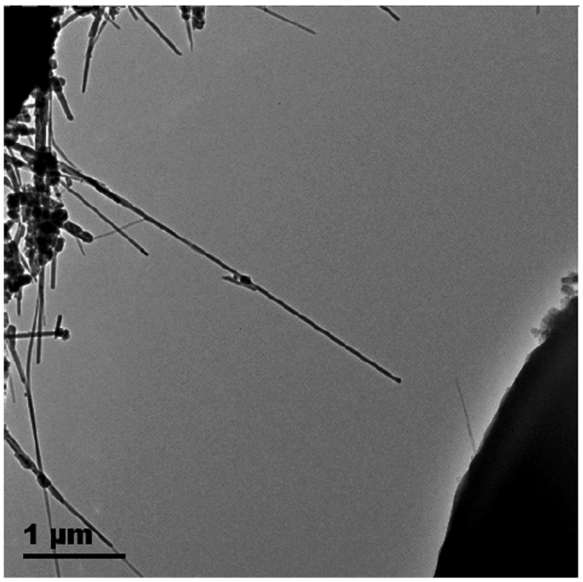

(b)

Fig. 5. Estimation of electrostatic forces (stiffness constant of AFM cantilever: 0.03 N/m). (a) Original state. (b) Bias voltage: 30 V.

real time. However, the applied actuating voltage makes it difficult, if not impossible, for electron microscopes to obtain real-time imaging because of spontaneous emission of electrons. Furthermore, electron-beam-induced contamination can cause interlayer locking, and the low bandwidth nature of electron microscopes is problematic. Here, two promising methods of position sensing for nanomotors are discussed: noncontact position sensing for cantilevered and middle-supported nanomotors using field emission, and contact position sensing for bridged nanomotors using interlayer resistance.

A. Noncontact Position Sensing With MWNTs

The position sensing configurations are shown schematically in Fig. 6. The field emission from a nanotube emitter is governed by the Fowler–Nordheim theory [30]

$$I_E = 1.54 \times 10^{-6} \frac{Al^2V^2}{G^2r^2\Phi} \exp\left(-6.79 \times 10^7 \frac{\Phi^{3/2}Gr}{Vl}\right) \quad (1)$$

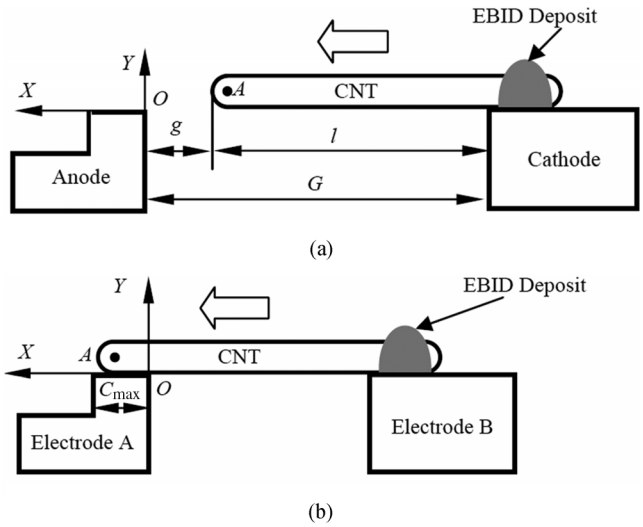

Fig. 6. Position sensing using CNTs. (a) Noncontact position sensing. (b) Contact position (sliding) sensing.

where I_{E} is the emission current (A); V is the applied voltage (V); Φ is the work function of nanotube tip (eV); r is the tip radius of curvature (i.e., the radius of the nanotube tip) (in centimeters); l is the protruding length of emitter (cm); G ($G = l + g$, g is the tip-anode distance) is the interelectrode distance (cm); A is the emission area [cm^2], and

$$\ln\frac{I_E}{V^2} = (-6.79 \times 10^7 \Phi^{3/2}\alpha r)\frac{1}{V} - \ln\frac{\alpha^2 r^2 \Phi}{1.54 \times 10^{-6} A} \quad (2)$$

where α is a parameter determined by the local geometric and electronic factors $\alpha = G/l$.

From (1), the emission current changes with the interelectrode gap G as

$$\frac{\partial I_E}{\partial G} = \left(-3.08 \times 10^{-6}\frac{Al^2V^2}{G^3r^2\Phi} - 104.57\frac{AlV^2\Phi^{1/2}}{G^2r}\right) \times \exp\left(-6.79 \times 10^7 \frac{\Phi^{3/2}Gr}{Vl}\right). \quad (3)$$

From (1) and (3) and for field emission ($G > l$) in the "near-field" (i.e., $G \approx l$ or $\alpha = G/l \approx 1$ and I_E becomes maximum and is inversely proportional to G so that better resolution is obtained). In a Fowler–Nordheim plot, this means a large inclination (see (2) for the coefficient of $1/V$). On the other hand, in a far field as $G \gg l$ or $\alpha = G/l \gg 1$, the resolution becomes worse. Experiments in [15] show that it is possible to obtain 100-nm resolution at room temperature in 10^{-4} Pa vacuum. Higher resolution can be obtained by stabilizing the emission current by baking the nanotube emitters and working at lower temperatures and in a higher vacuum.

B. Contact Position Sensing With MWNTs

Another position sensing technique is to use the nested tubes as sliding potentiometers or linear encoders. The interlayer resistance of telescoping nanotubes is promising for this purpose [18]. The outer layers can also be replaced with a plane. A nanotube sliding on an Au substrate (Fig. 7) yields an encouraging result as shown in Fig. 8. Contact sliding ($0 < G \leq l$ as shown in Fig. 6) is straightforward in principle. Under a constant bias V, the ohmic transport current I_T will change with the interelectrode distance or effective nanotube length G as $I_T = \pi V r^2/(\rho G)$ (ρ: resistivity). The resolution of the sliding

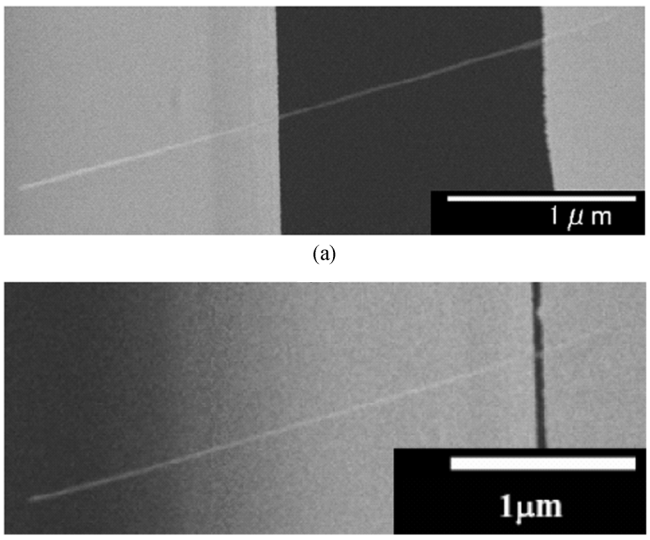

Fig. 7. Two positions of the nanotube-Au substrate sliding position sensor.

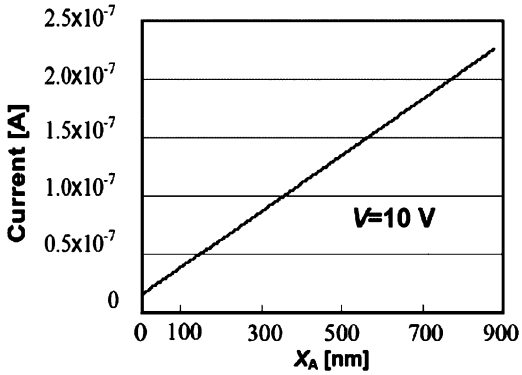

Fig. 8. Relation between the tip position of a nanotube and the current under 10-V constant bias.

sensor is found to be 0.24 nA/nm or 715 $\mathrm{k}\Omega$/nm. This is superior to the field emission mode. Excellent linearity also suggests easier calibration.

V. Integrated Devices and Potential Applications

From the view of fabrication, cantilevered telescoping MWNTs are superior and, therefore, the simplest position sensing method is field emission. Other possible linear servomotor designs include a bridged telescoping MWNT with a sliding potential meter, and a middle-supported MWNT with two field emission sensors.

The system configuration for a telescoping nanotube with field emission position feedback is shown in Fig. 9. An opened MWNT is fixed onto an AFM cantilever (acting as the cathode) by electron-beam-induced deposition (EBID) [31] on the right end of the structure. The tube is placed against a substrate serving as an anode. The interelectrode distance between the substrate and the AFM cantilever is indicated as G. The protruding length of the nanotube l will change Δl from its initial length l_0 as the electrostatic force between the core and the counter-electrode exceeds the sum of the interlayer friction and van der Waals forces between the core and the cathode. Hence,

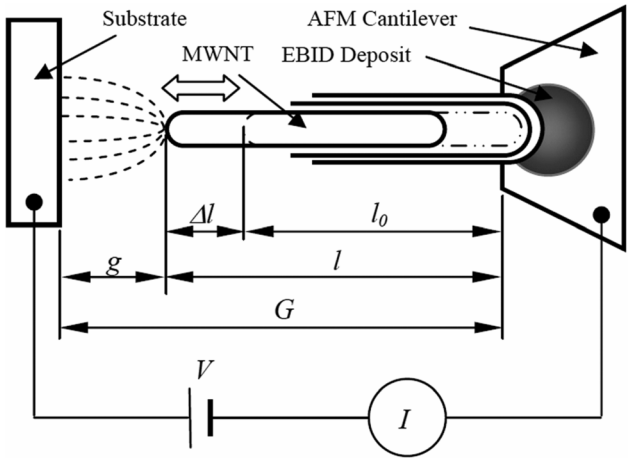

Fig. 9. Prismatic nanomotor with integrated field emission position sensing.

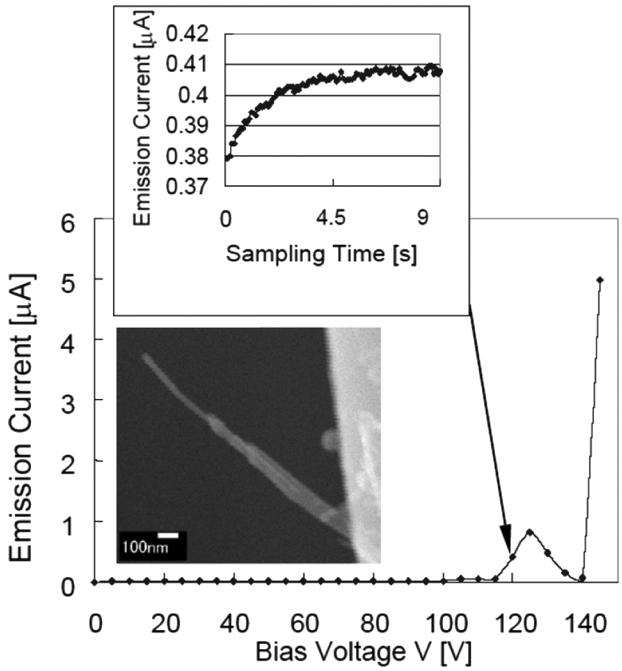

Fig. 10. Typical I–V curve of a telescoping nanotube as the interelectrode gap $G = 1000$ nm. The inset shows the change of emission current with time at 120 V.

the gap between the nanotube tip and the anode g will change whereas G remains constant.

Field emission is measured using the configuration shown in Fig. 9. Fig. 10 shows a typical I–V curve of a telescoping nanotube (see the inset micrograph of Fig. 10) when the interelectrode gap G is 1000 nm. Each point represents an average of 100 samples within a 9-s interval. The inset shows the change of emission current with time at a constant bias of 120 V. An obvious feature of this I-V curve different from conventional ones is the "kink" observed between 115 and 135 V.

Further investigation of the same tube under different gaps shows that the width of the "kink" can be shortened to 115 V–125 V as shown in Fig. 11. The Fowler–Nordheim plot shown in the inset of Fig. 11 is quite different from conventional linear plots. The knee has been discussed by Collins and Zettl [32],

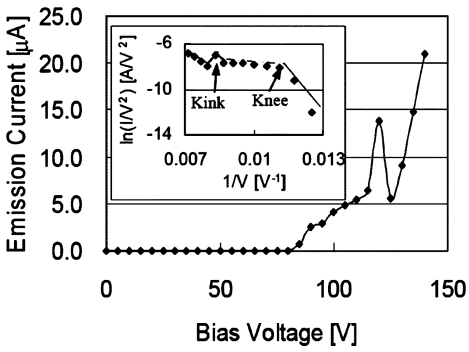

Fig. 11. Typical I–V curve of a telescoping nanotube as the interelectrode gap $G = 500$ nm.

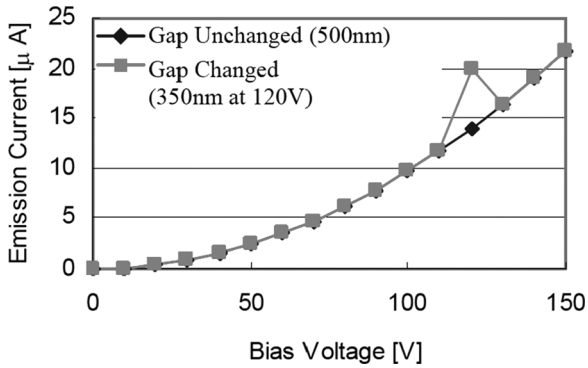

Fig. 12. Influence of the gap between CNT tip and anode on the emission current when bias voltage changes.

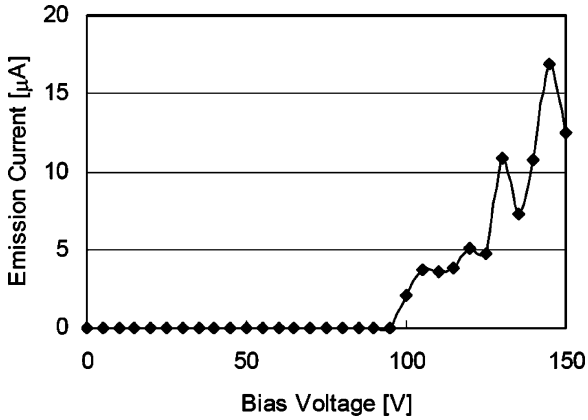

Fig. 13. Multiple "kinks" of the emission current.

whereas the "kink" with a large amplitude corresponding to that in the I–V curve has never been reported.

Fluctuations of emission current of conventional nanotube emitters have been found to be caused by headshaking, temperature change, vacuum alteration, or adsorption and desorption of molecules. Such fluctuations are random, such as the signal variation on the monotonic curve shown in the inset of Fig. 10. The relatively slow, long-term, reversible, and repeatable change with large amplitude is not due to these factors. Unfortunately, the applied bias voltage inhibits direct observation during the "kink" due to the side effect of the bias on the electron beam of the field emission scanning electron microscope used in the experiment.

Among all parameters, only the change in length of the nanotube or the gap between the CNT tip and the anode, and the voltage can induce the reversible and repeatable change of current if the interelectrode gap G remains unchanged. These changes can be expressed as

$$\frac{\partial I_E}{\partial l} = \left(3.08 \times 10^{-6} \frac{AlV^2}{G^2 r^2 \Phi} + 104.566 \frac{AV^2 \Phi^{1/2}}{Gr}\right) \times \exp\left(-6.79 \times 10^7 \frac{\Phi^{3/2} Gr}{Vl}\right) \quad (4)$$

and

$$\frac{\partial I_E}{\partial V} = \left(3.08 \times 10^{-6} \frac{Al^2 V}{G^2 r^2 \Phi} + 104.566 \frac{Al\Phi^{1/2}}{Gr}\right) \times \exp\left(-6.79 \times 10^7 \frac{\Phi^{3/2} Gr}{Vl}\right). \quad (5)$$

Fig. 12 shows a computed result of the resultant effect of these changes on the emission current under experimental conditions similar to those in Fig. 11. The similarity between Figs. 12 and 11 confirms that the length change (150 nm protruded at 120 V in Fig. 12) of the nanotube emitter is responsible (i.e., the telescoping motion of the tube causes the appearance of a "kink").

Multiple "kinks" are also observed as shown in Fig. 13. Because there is no apparent length change before and after the emission experiment, the appearance of the multiple fluctuations might be caused by telescoping motions between different layers (i.e., the peeling of the nanotube layer by layer from the innermost cores).

It should be noted that the telescoping system shown in Fig. 9 is unstable from a control perspective because of its positive feedback nature. As the nanotube tip approaches the anode, a larger emission current results and, hence, a stronger field, which will cause the core to continue extending until g is zero. In the process of extension, the current may become saturated and cause the protruding core to be shortened as shown in Fig. 14, as we have observed in nontelescoping nanotubes [28]. The unidirectional pullout of inner tubes has also been observed as shown in Fig. 15.

Of even more interest is that the core retracts from a stable position by either decreasing the bias voltage or from an external disturbance. This is caused by van der Waals forces and/or dielectrophoresis, depending on the conductivities of the layers and the coupling between layers of nanotubes, because the core offset induces axial van der Waals forces that can be several orders of magnitude larger than the interlayer friction. Hence, by controlling the applied voltage, it is possible to control the position of the core, and the field emission current can be used to detect the position, thus forming a closed-loop linear nanomotor.

VI. Conclusion

Nanoscale linear servomotors with integrated position sensing have been investigated from experimental, theoretical, and design perspectives. Prismatic motion has been realized by the interlayer motion of telescoping multiwalled carbon nanotubes. Noncontact and contact position sensing methods have been presented using both field emission and resistance change between an MWNT and a gold substrate during contact sliding

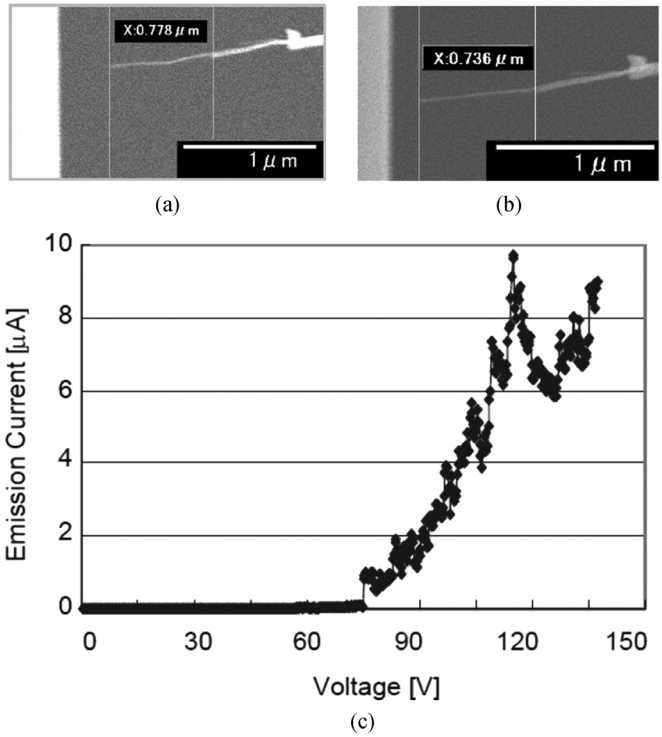

Fig. 14. Length change observed before and after field emission. (a) Before field emission; (b) after field emission; (c) I–V curve of field emission.

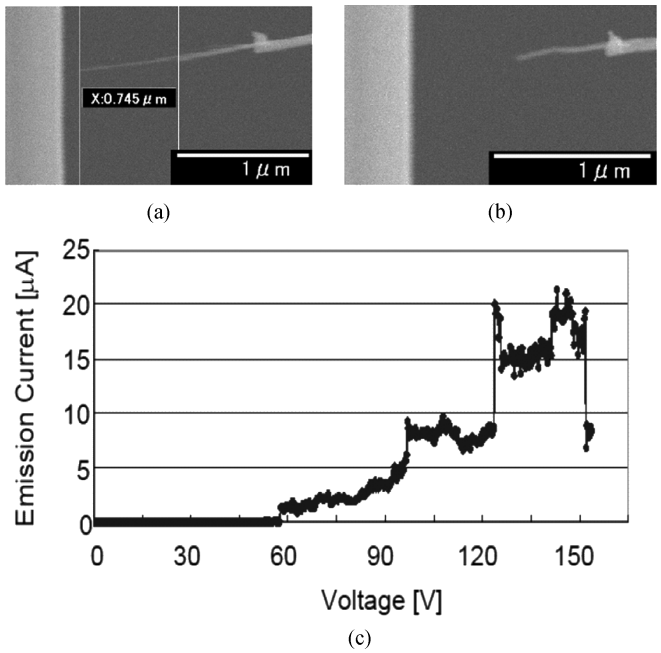

Fig. 15. Length change observed before and after field emission. (a) Before field emission, (b) after field emission, and (c) I–V curve of field emission.

movement. Experiments have shown the potential for high resolution nanometer scale precision. Actuation experiments have demonstrated the feasibility of a prismatic nanoservomotor with integrated position sensing based on field emission. A local "kink"-like fluctuation of emission current has been observed, which has been shown to be caused by the change of the protruding length of the nanotube core. The complete extension of the inner core has been observed and the necessary electrostatic force is calibrated to be tens of nano-Newtons for individual nanotubes—16.5 nN under a 30-V bias. Independent position sensing from electron microscope imaging suggests that the degradation of the motors by electron-beam-induced interlayer fixation can be avoided, and that a lower actuation voltage is sufficient to avoid shortening of the core by saturated emission currents. While fully servoed linear motors remain a challenge, these investigations demonstrate the possibility of fabricating linear servomotors in the nanometer scale with integrated position sensing.

ACKNOWLEDGMENT

The authors would like to thank Prof. Y. Saito of Nagoya University for providing the MWNTs.

REFERENCES

[1] V. Balzani, M. Venturi, and A. Credi, *Molecular Devices and Machines: A Journey Into the Nanoworld*, 1st ed. Weinheim, Germany: Wiley-VCH, 2003, pp. 269–277.
[2] K. E. Drexler, *Engine of Creation*, 1st ed. New York: Doubleday, 1986, p. 11.
[3] ——, *Nanosystems: Molecular Machinery, Manufacturing, & Computation*, 1st ed. New York: Wiley, 1992, pp. 273–319.
[4] S. Iijima, "Helical microtubules of graphitic carbon," *Nature*, vol. 354, pp. 56–58, 1991.
[5] A. M. Morales and C. M. Lieber, "A laser ablation method for the synthesis of crystalline semiconductor nanowires," *Science*, vol. 279, pp. 208–211, 1998.
[6] Z. W. Pan, Z. R. Dai, and Z. L. Wang, "Nanobelts of semiconducting oxides," *Science*, vol. 291, pp. 1947–1949, 2001.
[7] R. H. Baughman *et al.*, "Carbon nanotube actuators," *Science*, vol. 284, pp. 1340–1344, 1999.
[8] B. J. Landi *et al.*, "Single wall carbon nanotube-Nafion composite actuators," *Nano Lett.*, vol. 2, pp. 1329–1332, 2002.
[9] P. Poncharal, Z. L. Wang, D. Ugarte, and W. A. de Heer, "Electrostatic deflections and electromechanical resonances of carbon nanotubes," *Science*, vol. 283, pp. 1513–1516, 1999.
[10] P. Kim and C. M. Lieber, "Nanotube nanotweezers," *Science*, vol. 286, pp. 2148–2150, 1999.
[11] X. Y. Kong and Z. L. Wang, "Spontaneous polarization-induced nanohelixes, nanosprings, and nanorings of piezoelectric nanobelts," *Nano. Lett.*, vol. 3, pp. 1625–1631, 2003.
[12] A. M. Fennimore *et al.*, "Rotational actuators based on carbon nanotubes," *Nature*, vol. 424, pp. 408–410, 2003.
[13] G. Binnig, H. Rohrer, C. Gerber, and E. Weibel, "Surface studies by scanning tunneling microscopy," *Phys. Rev. Lett.*, vol. 49, pp. 57–61, 1982.
[14] G. Binnig, C. F. Quate, and C. Gerber, "Atomic force microscope," *Phys. Rev. Lett.*, vol. 56, pp. 93–96, 1986.
[15] F. Arai, P. Liu, L. X. Dong, and T. Fukuda, "Field emission property of individual carbon nanotubes and its applications," in *Proc. IEEE Int. Conf. Robotics Automation*, New Orleans, LA, Apr. 26–May 1, 2004, pp. 440–445.
[16] L. X. Dong, F. Arai, T. Fukuda, and B. J. Nelson, "Field emission of telescoping multi-walled carbon nanotubes," in *Proc. 4th IEEE Int. Conf. Nanotechnology*, Munich, Germany, Aug. 17–19, 2004.
[17] P. Liu, L. X. Dong, T. Fukuda, F. Arai, M. Nagai, and Y. Imaizumi, "Carbon nanotubes based position sensors," in *Proc. Int. Conf. Intelligent Mechatronics and Automation*, Chengdu, China, 2004, pp. 12–17.
[18] A. Hansson and S. Stafstro, "Intershell conductance in multiwall carbon nanotubes," *Phys. Rev. B*, vol. 67, no. 075406, 2003.
[19] J. Cumings and A. Zettl, "Low-friction nanoscale linear bearing realized from multiwall carbon nanotubes," *Science*, vol. 289, pp. 602–604, 2000.
[20] Q. S. Zheng and Q. Jiang, "Multiwalled carbon nanotubes as gigahertz oscillators," *Phys. Rev. Lett.*, vol. 88, no. 045503, 2002.
[21] J. L. Rivera, C. McCabe, and P. T. Cummings, "Oscillatory behavior of double-walled nanotubes under extension: a simple nanoscale damped spring," *Nano Lett.*, vol. 3, no. 8, pp. 1001–1005, 2003.
[22] M.-F. Yu, O. Lourie, M. J. Dyer, K. Moloni, T. F. Kelley, and R. S. Ruoff, "Strength and breaking mechanism of multiwalled carbon nanotubes under tensile load," *Science*, vol. 287, pp. 637–640, 2000.

[23] M. F. Yu, B. I. Yakobson, and R. S. Ruoff, "Controlled sliding and pullout of nested shells in individual multiwalled carbon nanotubes," *J. Phys. Chem. B*, vol. 104, pp. 8764–8767, 2000.
[24] S. C. Tsang, Y. K. Chen, P. J. F. Harris, and M. L. H. Green, "A simple chemical method of opening and filling carbon nanotubes," *Nature*, vol. 372, pp. 159–162, 1994.
[25] P. G. Collins, M. S. Arnold, and P. Avouris, "Engineering carbon nanotubes and nanotube circuits using electrical breakdown," *Science*, vol. 292, pp. 706–709, 2001.
[26] J. Cumings, P. G. Collins, and A. Zettl, "Peeling and sharpening multiwall nanotubes," *Nature*, vol. 406, p. 586, 2000.
[27] L. X. Dong, F. Arai, and T. Fukuda, "Three-dimensional nanoassembly of multi-walled carbon nanotubes through nanorobotic manipulations by using electron-beam-induced deposition," in *Proc. IEEE Conf. Nanotechnology*, 2001, pp. 93–98.
[28] T. Fukuda, F. Arai, and L. X. Dong, "Assembly of nanodevices with carbon nanotubes through nanorobotic manipulations (*Invited Paper*)," *Proc. IEEE*, vol. 91, no. 11, pp. 1803–1818, Nov. 2003.
[29] Q. S. Zheng, J. Z. Liu, and Q. Jiang, "Excess van der Waals inter-action energy of a multiwalled carbon nanotube with an extruded core and the induced core oscillation," *Phys. Rev. B*, vol. 65, 2002.
[30] R. H. Fowler and I. W. Nordheim, "Field emission in intense electric fields," *Proc. R. Soc. London Ser. A*, vol. 119, pp. 173–181, 1928.
[31] L. X. Dong, F. Arai, and T. Fukuda, "Electron-beam-induced deposition with carbon nanotube emitters," *Appl. Phys. Lett.*, vol. 81, no. 10, pp. 1919–1921, 2002.
[32] P. G. Collins and A. Zettl, "Unique characteristics of cold cathode carbon-nanotube-matrix field emitters," *Phys. Rev. B*, vol. 55, pp. 9391–9399, 1997.

Lixin Dong (S'01–M'03) received the B.S. and M.S. degrees in mechanical engineering from Xi'an University of Technology, Xi'an, China, in 1989 and 1992, respectively, and the Dr. Eng. degree in micro system engineering from Nagoya University, Nagoya, Japan, in 2003.

He was a Research Associate with the Department of Mechanical Engineering, Xi'an University of Technology, from 1992 to 1995; a Lecturer from 1995 to 1998: and since 1998, has been an Associate Professor. In 1995, he was a Visiting Researcher in the Department of Mechanical Engineering, Fukui University, Fukui, Japan. From 2003 to 2004, he was an Assistant Professor in the Department of Micro-Nano Systems Engineering, Nagoya University. Currently, he is a Senior Research Scientist in the Institute of Robotics and Intelligent Engineering, Swiss Federal Institute of Technology, Zürich, Switzerland. His research interests include nanorobotic manipulation, nanofabrication, nanoassembly, NEMS, and nanorobotics.

Bradley J. Nelson (M'90) received the B.S. degree in mechanical engineering from the University of Illinois at Urbana-Champaign in 1984, the M.S. degree in mechanical engineering from the University of Minnesota, Minneapolis, in 1987, and the Ph.D. degree in robotics from the School of Computer Science, Carnegie Mellon University, Pittsburgh, PA, in 1995.

Currently, he is the Professor of Robotics and Intelligent Systems with ETH-Zürich, Zürich, Switzerland and is Director of IRIS and Head of the Department of Mechanical and Process Engineering (D-MAVT). He was an Engineer with Honeywell, Minneapolis, MN, and Motorola, Bothell, WA, and was a U.S. Peace Corps Volunteer, Botswana, Africa. In 1995, he became Assistant Professor with the University of Illinois at Chicago, Associate Professor at the University of Minnesota in 1998, and Professor at ETH-Zürich in 2002. His primary research direction is in extending robotics research into emerging areas of science and engineering. His most recent scientific contributions have been in the area of microrobotics, biomicrorobotics, and nanorobotics, including efforts in robotic micromanipulation, microassembly, microelectromechanical systems (MEMS) (sensors and actuators), mechanical manipulation of biological cells and tissue, and nanoelectromechanical systems (NEMS). He has also contributed to the fields of visual servoing, force control, sensor integration, and web-based control and programming of robots.

Dr. Nelson has been awarded a McKnight Land-Grant Professorship and is a recipient of the Office of Naval Research Young Investigator Award, the National Science Foundation Faculty Early Career Development (CAREER) Award, the McKnight Presidential Fellows Award, and the Bronze Tablet. He was elected as a Robotics and Automation Society Distinguished Lecturer in 2003 and received the Best Conference Paper Award at the IEEE 2004 International Conference on Robotics and Automation. He was named to the 2005 "Scientific American 50," Scientific American magazine's annual list that recognizes outstanding acts of leadership in science and technology from the past year. He serves on or has been a member of the editorial boards of the IEEE TRANSACTION ON ROBOTICS, the *Journal of Micromechatronics*, the *Journal of Optomechatronics*, and the *IEEE Robotics and Automation Magazine*. He has chaired several international workshops and conferences.

Toshio Fukuda (M'83–SM'93–F'95) received the B.A. degree from Waseda University, Tokyo, Japan, in 1971, and the M.S and Dr.Eng. degrees from the University of Tokyo, Tokyo, Japan, in 1973 and 1977, respectively.

In 1977, he joined the National Mechanical Engineering Laboratory. In 1982, he joined the Science University of Tokyo, Tokyo, Japan, and then joined Nagoya University, Nagoya, Japan, in 1989. Currently, he is a Professor in the Department of Micro/Nano Systems Engineering at Nagoya University, where he is mainly involved in the research fields of intelligent robotic systems, cellular robotic systems, mechatronics, and micro and nanorobotics.

Dr. Fukuda was President of the IEEE Robotics and Automation Society from 1998 to 1999, Director of the IEEE Division X, Systems and Control from 2001 to 2002, President of the IEEE Nanotechnology Council from 2002 to 2003, and Editor-in-Chief of IEEE/ASME TRANSACTIONS ON MECHATRONICS from 2000 to 2002. Currently, he is President of the Japan Society for Fuzzy Theory and Intelligent Informatics (SOFT).

Fumihito Arai (M'91) received the Dr. engineering degree from Nagoya University, Nagoya, Japan, in 1993.

In 1989, he joined Nagoya University as a Research Associate and became Associate Professor in the Department of Micro-Nano Systems Engineering in 1998, involved in the research fields of micro and nanorobotics and their application to the micro and nanoassembly and bioautomation, microelectromechanical systems (MEMS) and nanoelectromechanical systems (NEMS), microsensors, microactuators, intelligent robotic systems, and intelligent human–machine interface.